Arab J Sci Eng (2017) 42:1765–1773
DOI 10.1007/s13369-016-2305-1

RESEARCH ARTICLE - MECHANICAL ENGINEERING

Fiber Laser Welding of Thin Nickel Sheets in Air and Water Medium

Vikash Kumar[1] · **Manowar Hussain**[1] · **Mohammad Shahid Raza**[1] · **Alok Kumar Das**[1] · **N. K. Singh**[1]

Received: 29 December 2015 / Accepted: 22 August 2016 / Published online: 30 August 2016

Abstract In the present research, fiber laser beam welding (FLBW) of thin nickel sheets in two different mediums, i.e., air and water, has been investigated. In air medium, the fiber laser welding operations are performed at different laser powers (60, 80 and 100 W) and scanning speeds (40, 60 and 80 mm/min). Underwater welding operations have also been investigated at three different laser powers (330, 350 and 370 W) and two different scanning speeds (20 and 40 mm/min). The results show that welding of Ni sheet with higher laser power results in prominent heat-affected zone, increase in both microhardness and wt% of oxide formation in the weldment in both air and water medium. It is found that the increase in microhardness of weldment leads to the reduction in grain size. The heat-affected zone is reduced when scanning speed is increased. The wt% of oxygen increases with an increase in power during FLBW operation at constant scanning speed, and the oxide formation can be controlled by varying the laser power and scanning speed. The welding medium has significant influences on the properties of the weldments.

Keywords Microhardness · Microstructure · Heat-affected zone (HAZ) · Microwelding

✉ Alok Kumar Das
eralok@yahoo.co.in

[1] Mechanical Engineering Department, Indian school of Mines, Dhanbad, Jharkhand, India

1 Introduction

Thin nickel sheets are commonly used in many industries for producing products such as medical and electronics components, aircraft and missile components, food handling systems and heat exchangers, due to its high corrosion resistance and superior electrical and thermal conductivity than its superalloys. Nickel-based superalloys like IN-738 and K418 are developed mainly for high-temperature applications, excellent elevated temperature creep-rupture strength and for superior corrosion resistance in high-temperature applications [1,2]. Although, a considerable number of welding processes [3] and hybrid welding processes [4] have been performed and investigated for nickel-based superalloys, very less literature is available on the welding of thin nickel sheet using a fiber laser. Welding in water medium has been reported to carry out the underwater maintenance in various industries such as in ship industries and nuclear power plants. [5,6]. Underwater laser beam welding processes face two common difficulties: first, the absorption of laser power in water and, second, the effect of water on mechanical and morphological behavior of the weldment [7]. The mechanical and microstructural properties of a weldment are dependent on the heating and cooling rate [8]. Laser power and welding speed are the main parameters which affect the material properties of the weldment [9]. Low power and high scanning speed is preferred for laser welding to minimize the residual stress in the weld zone [10–12]. Underwater fiber laser welding is feasible due to the low absorptivity ($0.014\,mm^{-1}$) of the fiber laser (1.070μm wavelength) in water medium [13–15]. Laser welding is a high-power density, low heat-input process with specific advantages over traditional welding processes. These include narrow heat-affected zone, high welding speed, low distortion of the work piece [3], single-pass thick section welding capability,

enhanced design flexibility and ease of automation. Welding without filler material is one of the features of laser welding which offers distinct advantages [16–19]. Welding of thin sheet metals is a big challenge for various industries, mainly due to two problems: one is very fine edge requirement, and the other is the fixture for holding thin sheets with perfect alignment, since thermal distortion during laser welding may cause a joint gap or mismatching. In terms of weldability of metallic materials, fiber laser has various advantages, such as high-energy absorption rate due to low reflectivity, a high welding speed and a low residual stress compared to CO_2 laser. Thus, the application of fiber laser to weld the metallic parts is increasing steadily and now it is widely implemented in various industrial applications.

In this paper, lap joints from nickel sheets of 0.23 mm thickness have been prepared by using fiber laser, in both air and water medium, and various characterization techniques have been carried out to observe the microstructure, heat-affected zone (HAZ), weight percentage of oxygen content and microhardness of the weldments.

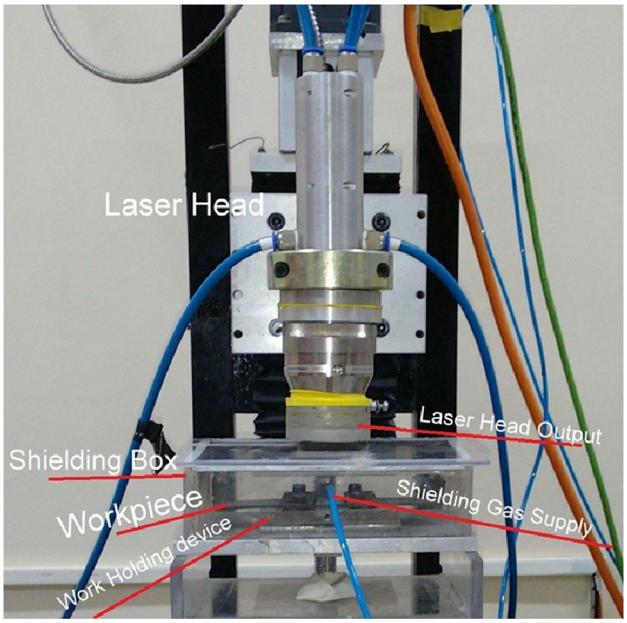

Fig. 1 Fiber laser work station with an arrangement for welding operation

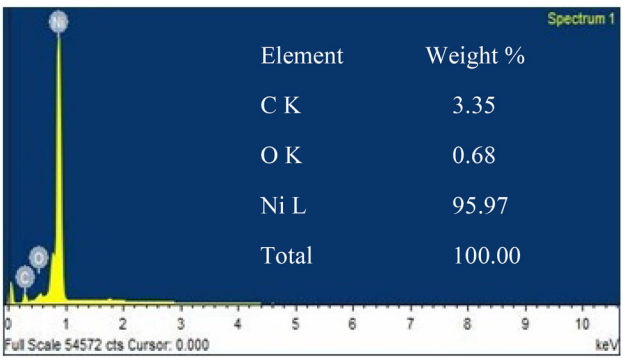

Fig. 2 EDS analysis of pure nickel sheet

2 Experimental Procedure

2.1 Experimental Setup Preparation

A continuous wave fiber laser work station was used to carry out the welding experiments. The setup consists of fiber laser source (make: SPI, UK, model: SM-S00051) with maximum power 400 W and wavelength 1070 nm. A laser welding head (make: Precitec, Germany) with 80 mm focal length is retrofitted to a 3 axis CNC work table. The work holding vice was fabricated from perspex sheet (6 mm thickness), to hold the nickel sheet during the welding experiments. The thin nickel sheets were mounted in the work holding vice so as to reduce the angular deformation due to the holding pressure. The whole arrangement was kept in a closed welding chamber, and the argon gas was purged for few moments (time: 30 s) before conducting the welding experiments, to prevent the formation of metal oxide. The experimental setup arrangement is shown in Fig. 1.

2.2 Preparation of Work Piece

Nickel sheets with dimensions 20 mm × 10 mm × 0.23 mm were selected for laser welding experiments. Wire-EDM process with low energy was used to cut the nickel strips [20] from pure nickel sheet as very fine edges are required for the laser welding process. Figure 2 represents the results of EDS examination of the pure nickel sheet. After cutting, the strips were cleaned in an acetone bath which was exposed to ultrasonic vibration. Then, the sheets were dried and mounted in the fabricated welding fixture so as to minimize the air gap between the two lapping edges. In underwater welding process, a water level of 1 mm height was maintained during the welding process.

2.3 Experimentation

The fiber laser beam welding (FLBW) experiments were carried out in both air and water medium. The laser power and scanning speed have been taken as variable input parameters keeping other parameters, i.e., standoff distance, inert gas flow rate as constant. Table 1 represents the parameter settings for different experiments in air medium. The pure argon gas with a flow rate of 20 l/min was purged in air

Table 1 Summary of the experimental parameter settings in air medium

Sample No.	Power (W)	Scanning speed (mm/min)	Spot size (mm)	HAZ (μm)	wt% of oxygen	Microhardness (HV)
1	60	40	0.4	532.22	8.23	104.1
2		60		433.33	5.98	117.1
3		80		347.83	3.06	124.5
4	80	40		652.66	19.36	112.5
5		60		487.06	17.53	126.3
6		80		371.83	9.35	136.3
7	100	40		1009.8	24.16	118.8
8		60		815.33	19.58	132.4
9		80		519.8	21.26	164.8

Table 2 Summary of experimental welding parameters in water medium

Sample No.	Power (W)	Feed (mm/min)	Water depth (mm)	HAZ (μm)	wt% of oxygen	Microhardness (HV)
1	330	20	1	454.02	13.82	118.4
2		40		287.73	10.35	128.3
3	350	20		460	14.68	124.6
4		40		338.1	11.44	132.8
5	370	20		535.12	20.33	128
6		40		558.55	18.72	156.2

medium to reduce the oxide formation during the welding operation. In water medium, comparatively higher power and low scanning speed was selected, and the details of the parameter settings are presented in Table 2. Above parameters are selected in order to obtain the full welding penetration along the thickness of the joints. The argon gas was purged at flow rate of 5 l/min in water medium to prevent the entry of water vapor into the welding head. After the welding operations, the weldment was polished to mirror finishing by a polishing machine (make: Chennai metko). Then, the weldment is etched using an etchant which is composed of equal parts of HCL, HNO_3 and acetic acid. Different characterization techniques were followed to study the heat-affected zone (HAZ), microstructure, microhardness and weight percentage (wt%) of oxygen formation in the weldments. Metallurgical microscope was used for measuring the width of HAZ of the welded samples and to observe the physical features of the weld zone and presence of surface and under surface defects (such as blow holes, pin holes, and porosity). For microstructure of the weldments, FESEM (SUPRA 55 Germany with Air Lock, EDS, EBSD) was used and EDS analysis was carried out on top surface of the weld bead for finding the weight percentage of oxygen formation in the weldment. Microhardness of weldments was measured on the top surface of weldment using Vickers microhardness tester (Econonet VH-1 MD, MAKE: Chennai Metco, India).

3 Results and Discussion

3.1 Analysis of Laser Welding of Nickel Sheets in Air Medium

3.1.1 Influence of Laser Power and Scanning Speed on the Width of Heat-Affected Zone (HAZ)

After welding, the prepared samples were cleaned and polished to observe the microstructural changes in the weld zone. Figure 3 indicates that the optical images of the three different welded samples showing the microstructure at the weld zone and the different zones are shown in the figure. It is seen that the grain sizes are different in base metal, weld bead and HAZ. The average value of the width of HAZ is taken into account. With increase in the feed rate or scanning speed, the width of HAZ decreases at constant power [21]. At a constant power level, with the increase in the feed rate the amount of heat generated on the weldment reduces whereby width of HAZ is reduced which means the welding of Ni sheets follow the same trend as other material do with laser welding. Figure 4 shows the influence of laser power and laser beam scanning speed on the width of HAZ which is formed during laser welding operation. It has been reported that in the welding of different metals, i.e., steel, Ti alloys, with the increase in laser power at constant scanning speed, the width of heat-affected zone increases, and with increase in scanning speed

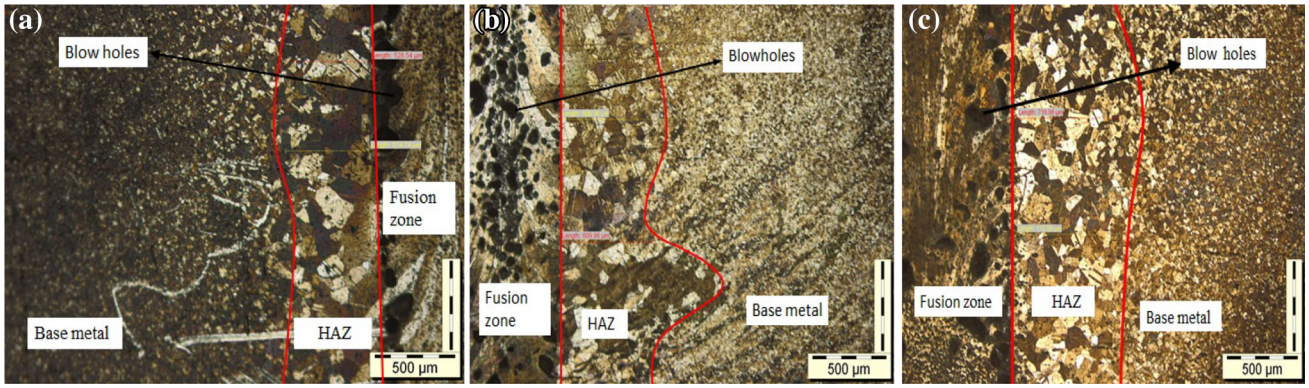

Fig. 3 Optical microscope images for three different laser parameter combinations after polishing and etching. **a** 60 W, 80 mm/min, **b** 60 W, 60 mm/min and **c** 60 W, 40 mm/min

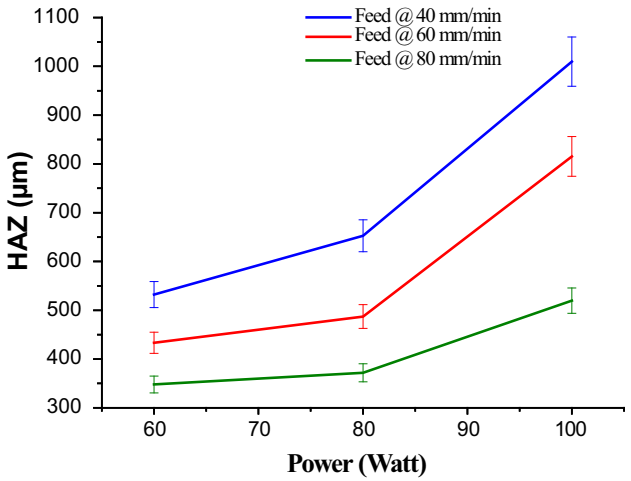

Fig. 4 Variation of HAZ with laser power for different scanning speed

at constant laser power, HAZ reduces [22–24]. Laser power and scanning speed have a vital role on the HAZ. With the increase in laser power at constant scanning speed, the temperature of workpiece rises to its melting point and the metal sheets get welded. With further increase in laser power, the temperature of metal nearby the weld zone increases, and thus, the width of HAZ increases [25].

3.1.2 *Effect of Laser Power on Weight Percentage of Oxygen Content in the Weld Zone*

During the welding process, constant argon gas flow rate was maintained to shield the surface and reduce the oxide formation on the weld bead. But, after welding operation it was observed that the color of surface material near the weld bead was different from the parent material (Fig. 5). It may be due to the formation of oxide layer, so the EDS examination was carried out to see the presence oxygen in the colored surface. Figure 6 represents the results of EDS test on one of the prepared samples. Similarly, for each sample the wt% of oxygen content was tested through EDS examination. Figure 7 represents the variation in wt% of oxygen content with different combinations of laser power and scanning speed.

The presence of oxygen is directly related to the oxide formation on the surface. Oxide formation in the weldment reduces the strength and also increases the hardness of joint of metal sheets. As the laser power increases, the temperature

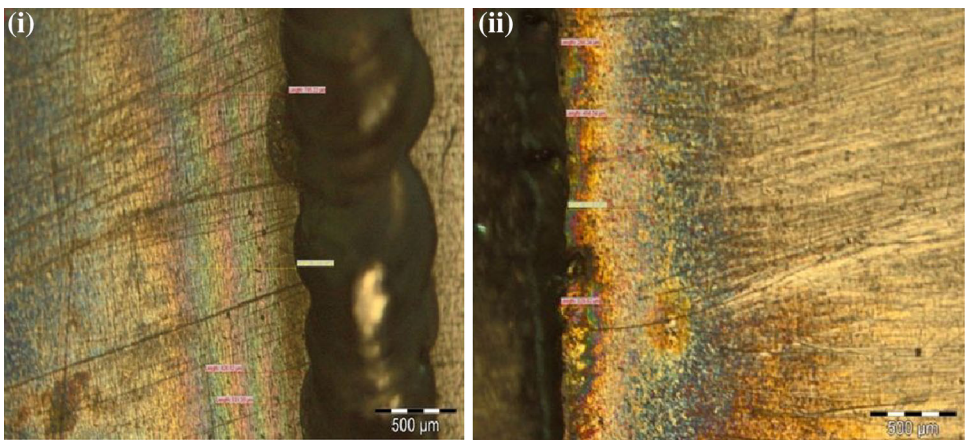

Fig. 5 Optical microscope images of oxide layer for two different samples at **a** 80 W, 40 mm/min and **b** 80 W, 100 mm/min

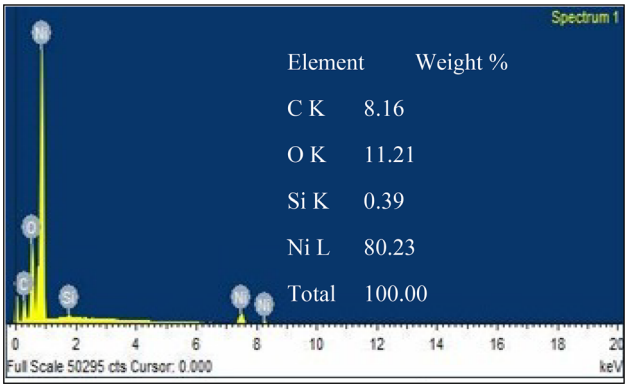

Fig. 6 wt% of oxygen in the weld zone prepared with laser power of 80 W and scanning speed of 80 mm/min

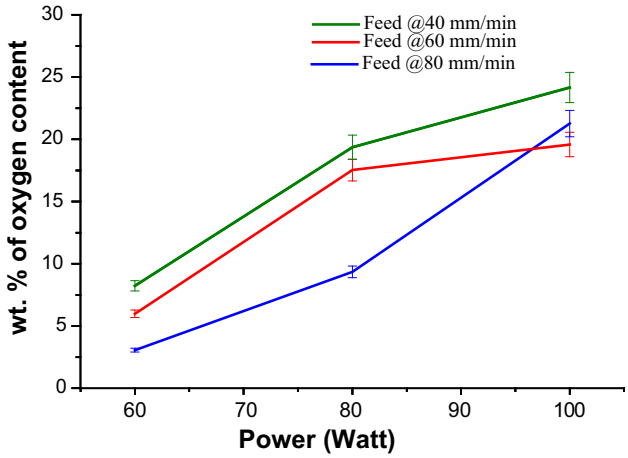

Fig. 7 Variation of wt% of oxygen in weld bead with power

of the samples to be welded goes high which activates the nickel to react with the atmospheric oxygen and leads to the increase in oxide formation.

3.1.3 Effect of Laser Power on Microhardness

The sample was held in the vice of the Vickers microhardness testing machine. The indentations were carried out along the weld bead, and the values were recorded. During the testing, a weight of 0.5 kg was applied for dwell time of 10 s. For each sample, 10 indentations were performed and average value was considered. Figure 8 shows the variation of microhardness with laser power. As the power increases, the microhardness increases at constant scanning speed. It can be justified by the Newton's law of cooling that states that convection heat transfer increases with increase in temperature difference between weld bead and surrounding; therefore, with increase in welding power, cooling rate of weldment increases, whereby microhardness of welded part increases [26]. Increase in hardness value of the weld joint would result in a decrease in the load-bearing capacity of the joint [27].

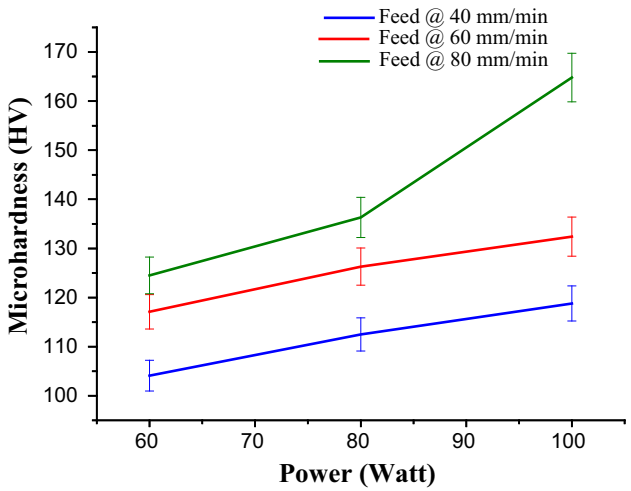

Fig. 8 Variation of Vickers microhardness (HV) with power (W) for three different scanning speeds

Average microhardness of pure Nickel sheet of thickness 0.23 mm is 96.9 HV, so from Table 1 it is observed that the microhardness values in the weld bead are increased significantly after welding. FESEM images (Fig. 9) and the microhardness data in Table 1 prove that microhardness of sample increases as the grain size reduces.

3.2 Laser Welding of Ni Sheet in Water Medium

Underwater lap welding of thin nickel sheet is a very challenging job. Comparing with the other underwater welding methods, underwater fiber laser welding provides remarkably low heat input, high cooling rate, narrow HAZ and produces low residual stress. These properties are of prime importance in underwater welding processes. In addition, fiber laser beam can be easily transmitted to any positions thorough fiber optics. The process is easy to control and flexible for precise repair welding. In general, two aspects should be considered for the assurance of weld quality in underwater LBW: one being the effect of water on the metallurgical behavior of the materials to be welded and the other being the absorption of laser beam in water medium.

3.2.1 Effect of Laser Power and Scanning Speed on the Width of HAZ

Figure 10 represents the plot for influence of laser power on the width of heat-affected zone (HAZ) in underwater welding. From the figure, it is clear that as the power increases at constant scanning speed, the heat-affected zone increases. With increase in power, the temperature of sample increases, whereby HAZ increases. The prepared samples were polished and etched with a standard etchant (solution containing equal proportion of HCl, HNO_3 and acetic acid) to examine

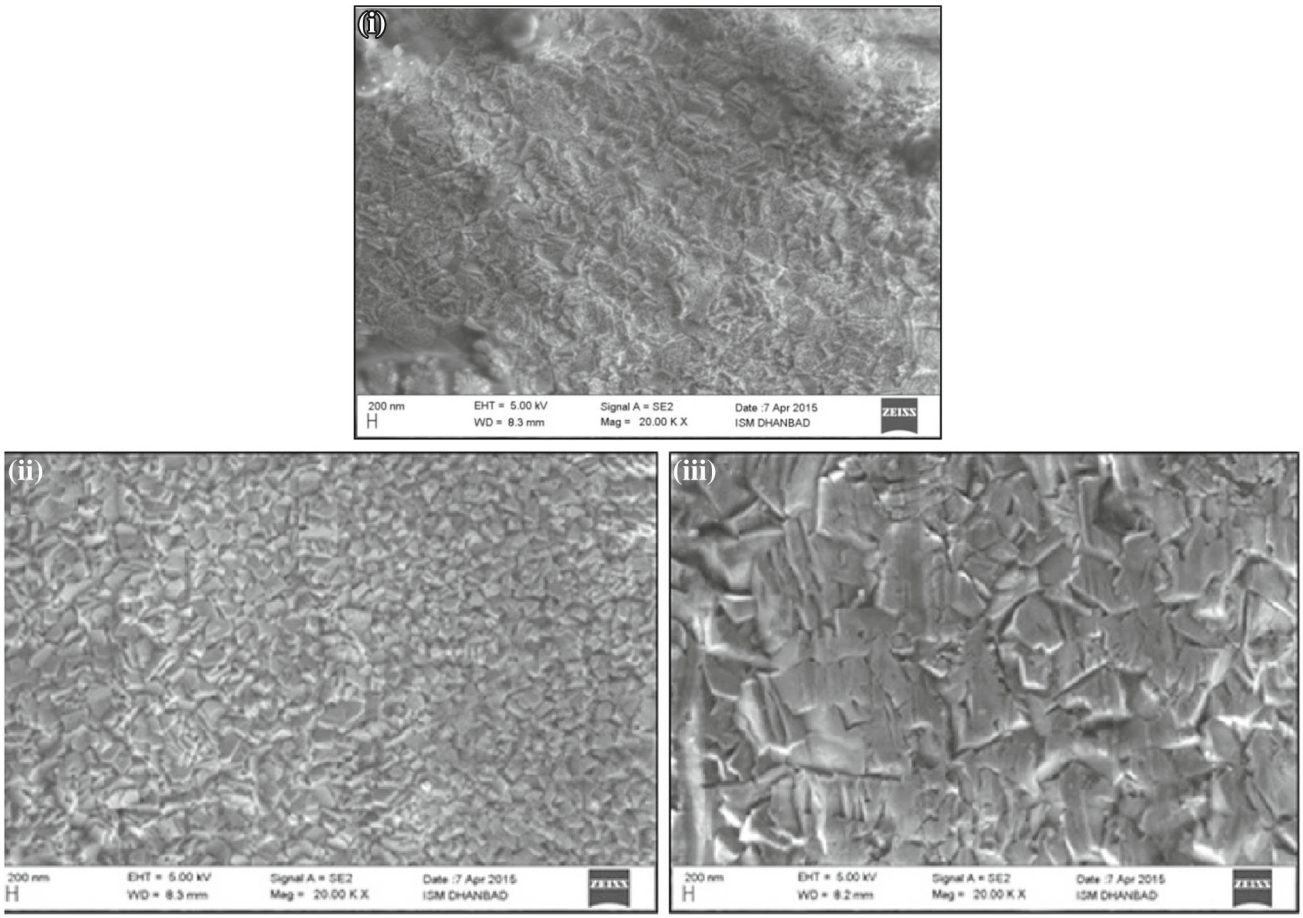

Fig. 9 FESEM Images of the weld zone at different parameter settings **a** 100 W, 40 mm/min, **b** 80 W, 40 mm/min and **c** 60 W, 40 mm/min

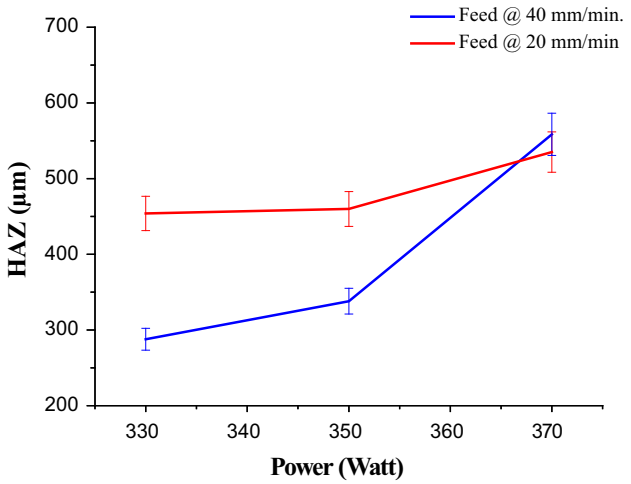

Fig. 10 Variation of HAZ with Power for different scanning speed in underwater medium FLBW

the microstructure changes in the welded zone. Few of the optical images are shown in Fig. 11. Table 2 shows the width of HAZ with variation of laser power and scanning speed. Most of the laser beam power was lost in heating the sample up to its melting temperature because water was getting evaporated and prevents the rise in temperature of the sample. With further increase in power, the temperature of material nearby the weld zone increases due to which the width of HAZ increases.

3.2.2 Effect of Laser Power on wt% of Oxygen Content

EDS analysis of the prepared samples was carried out to observe the percentage of oxygen present in the surface. Figure 12 shows the variation of oxygen content in the weld bead with laser power. The presence of oxygen in the weld bead is a clear indication of the formation of metal oxide on the surface. Figure 13 indicates the optical images of few of the weld bead which shows the change in color which may be due to the oxide formation, as it is removed after light polishing. The main reason behind the oxide formation is the increase in the temperature of metal surface, leading to oxidation reaction and formation of nickel oxide. The probable chemical reactions are as follows.

$$2H_2O \rightarrow 2H_2 + O_2 \quad \text{(Breaking of water)}$$

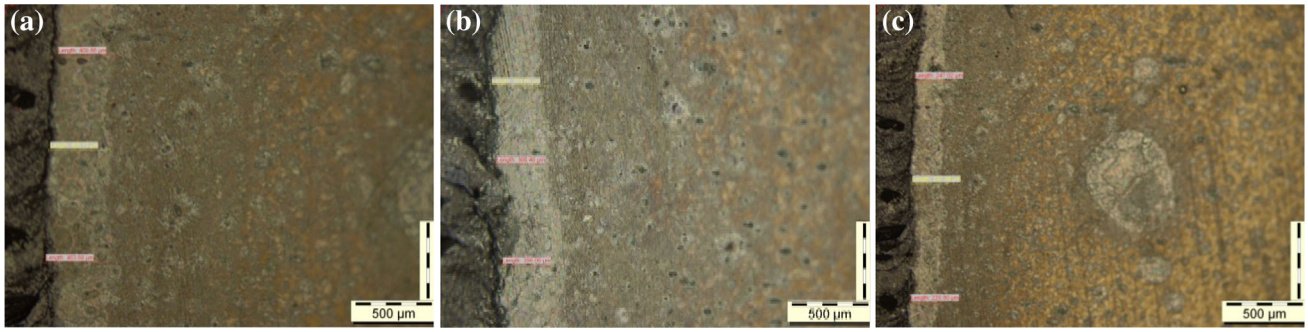

Fig. 11 Optical images of underwater welding for three different laser parameter combinations after polishing and etching. **a** 370 W, 40 mm/min, **b** 350 W, 40 mm/min and **c** 330 W, 40 mm/min

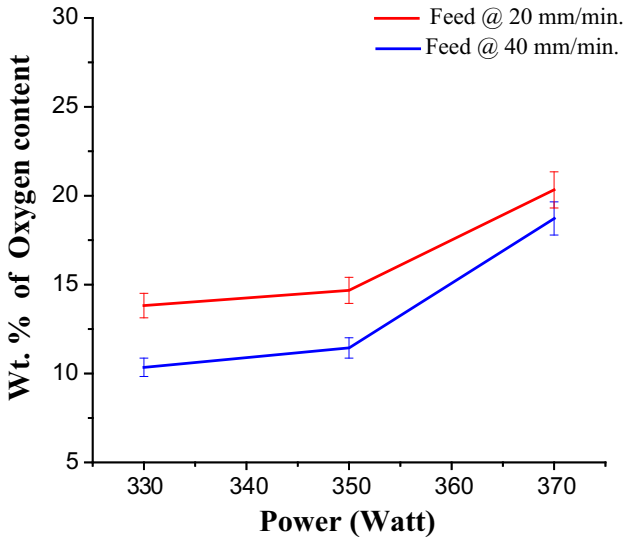

Fig. 12 Variation of wt% of oxide formation with laser power at different scanning speeds

$O_2 \rightarrow 2O$ (Nascent oxygen)

$3Ni + 4O \rightarrow NiO + Ni_2O_3$ (Ni Oxides)

3.2.3 Effects of Laser Power on Microhardness

Vickers microhardness testing machine was used to measure the microhardness in which a weight of 0.5 kg was applied for the dwell time of 10 s. Figure 14 represents the variation of microhardness with laser power. Analysis of microhardness value of welded sample in both medium shows that change in microhardness in case of water is higher as compared to air medium as instant quenching action is occurred, while welding is performed in the water medium. During the operation, water evaporates and forms water vapor, and further, the formation of hydrogen and oxygen molecules takes place due to the high temperature. These oxygen molecules react with heated surface and forms oxide. Change in grain size can be observed from FESEM images which indicate that the laser power has significant influence on microhardness as shown in Fig. 15.

4 Comparison of Results Obtained in Air and Water Medium

The use of water medium causes a substantial improvement in the morphological as well as microstructure of the weld-

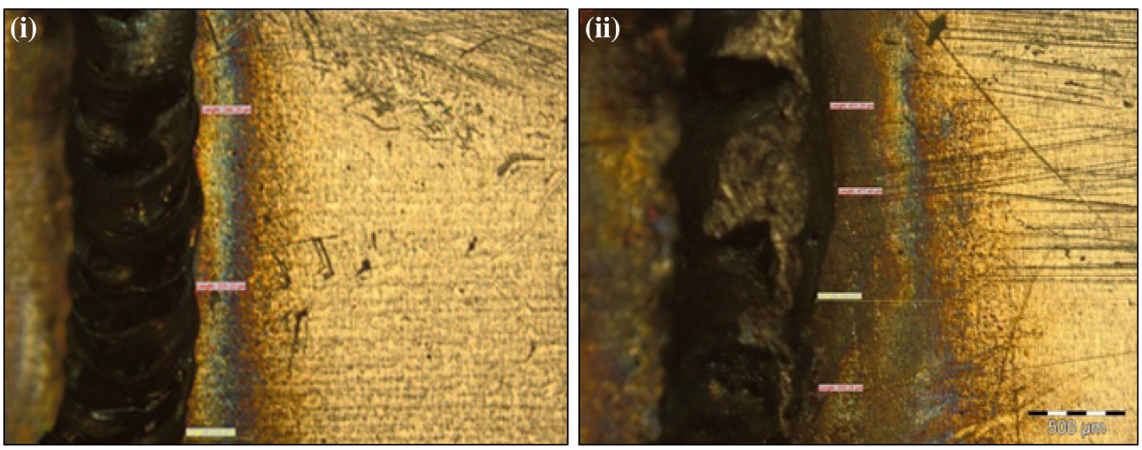

Fig. 13 Images of oxide layer formation for underwater FLBW samples at **a** 330 W, 20 mm/min and **b** 370 W, 20 mm/min

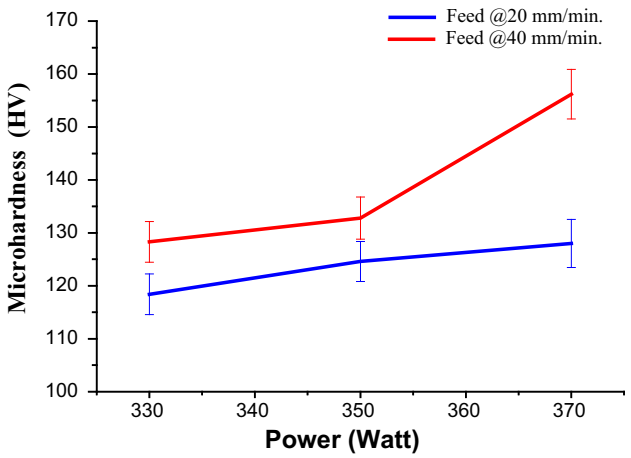

Fig. 14 Variation in Vickers microhardness with laser power at different scanning speeds

ment. The physical defects like blow hole are common in case of welding. Previous researchers have tried to minimize the blow holes through different parameter settings [28,29]. The presence of water medium causes the reduction in the formation of blow holes as shown in Fig. 11 in comparison with that of air medium as shown in Fig. 3. In air medium, the formation of spatter is observed which leads to the loss of metal and the molten metal in the melt pole becomes insufficient in filling up the empty space created during welding [28]. But in case of liquid medium the presence of liquid prevents the loss due to spatter which leads to better weld beads. FESEM images (Figs. 9, 15) show the similar results for the welding in both air and water medium. The grain size reduces as laser power increases. It can be due to the high-temperature gain in the weld pool and subsequently high rate of cooling causing finer grain formation. The width of HAZ in water medium is smaller than that of air medium because of different values of heat transfer coefficient of air and water at nickel surface. For some parameters, the width of HAZ in water medium is higher in comparison with air medium which may be due to the parameters value at which welding has done.

Welding in water medium leads to the increase in oxide formation in comparison with air medium. In SEM images Fig. 15, white dots figure out the presence of oxides which is comparatively less in SEM images in Fig. 9. Increase in oxide formation is due to the vaporization of water molecules on the work piece.

Microhardness of any metals in LBW process is highly dependent on the laser power, scanning speed as well as surrounding medium. Cooling rate in case of water medium is higher than in air; therefore, the microhardness is more in comparison with air medium. Since experiment was performed on different parameters of power and scanning speed for two mediums, so it is not justified to compare the microhardness values on the basis of these two parameters, i.e., power and scanning speed.

5 Conclusion

A number of experiments were performed to prepare lap joints of thin (0.23 mm thickness) nickel sheets using continuous wave fiber laser in both air and water medium. The experiments were conducted by varying two parameters such as laser power and scanning speed, while other experimental parameters were kept at constant level. Few of the mechanical and metallurgical properties of the weld beads were investigated. From the experimental observation and characterization of the weld beads, the following conclusion may be drawn.

The width of HAZ increases with the increase in laser power in both air and water medium at constant welding speed. Further, with the increase in welding speed at constant laser power the width of HAZ reduces. The slope of the plot for width of HAZ Vs laser power is low at the low power level and the wt% of oxide formation increases with increase in

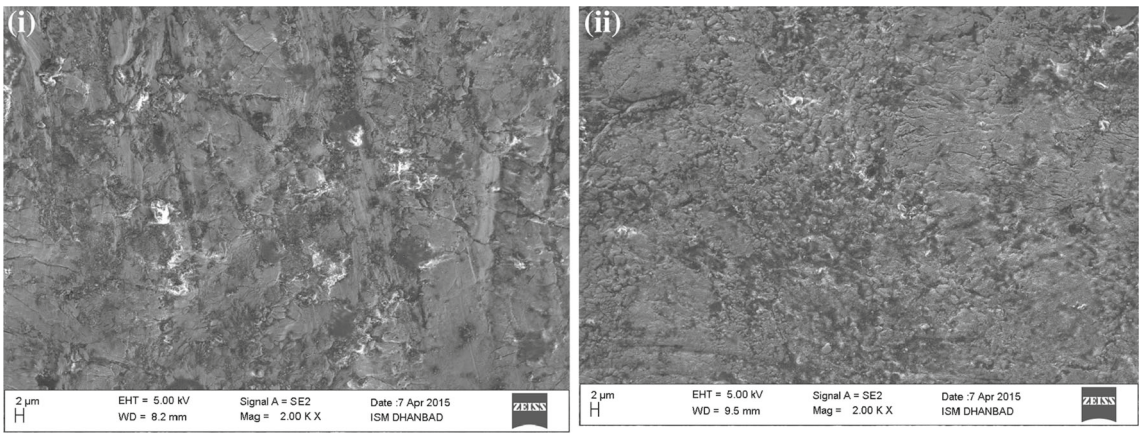

Fig. 15 FESEM images of underwater FLBW samples at **a** 330 W, 20 mm/min and **b** 370 W, 20 mm/min

laser power in both air and water medium at constant welding speed. So, it is suggested that optimum laser power may be selected without affecting the weld quality, for achieving the narrow HAZ and minimum level of formation of metal oxide.

The value of microhardness of the weld zone increases in both the medium as compared to the parent surface, when laser power increases while maintaining the constant scanning speed.

The formation of blow holes in water medium is very low in comparison with air medium, so the underwater welding of thin metal sheets may be a preferred choice for many industries. However, further investigations are required on the underwater welding of thin metal sheets.

References

1. Chiang, M.F.; Chen, C.: Induction-assisted laser welding of IN-738 nickel-base superalloy. Mater. Chem. Phys. **114**, 415–419 (2009)
2. Pang, M.; Yu, G.; Wang, H.H.; Zheng, C.Y.: Microstructure study of laser welding cast nickel-based superalloy K418. J. Mater. Process. Technol. **207**, 271–275 (2008)
3. Huang, H.; Wang, J.; Li, L.; Ma, N.: Prediction of laser welding induced deformation in thin sheets by efficient numerical modeling. J. Mater. Process. Technol. **227**, 117–128 (2016)
4. Arias, J.L.; Romero, P.; Bandewynckele, A.; Vázquez, J.: Laser-TIG hybrid welding of very thin austenitic stainless steel sheets. In: Proceedings of the 24th International Conference on Applications of Lasers and Electro-Optics, Miami, USA, pp. 104–107 (2005)
5. Jia, C.; Zhang, T.; Maksimov, S.Y.; Yuan, X.: Spectroscopic analysis of the arc plasma of underwater wet flux-cored arc welding. J. Mater. Process. Technol. **213**(8), 1370–1377 (2013)
6. Shi, Y.; Wang, G.; Liu, C.: Study on mini-cap local dry underwater flux-cored arc welding and online control of weld penetration. In: The Twentieth International Offshore and Polar Engineering Conference. International Society of Offshore and Polar Engineers (2010)
7. Zhang, X.; Chen, W.; Ashida, E.; Matsuda, F.: Metallurgical and mechanical properties of underwater laser welds of stainless steel. J. Mater. Sci. Technol. **19**(5), 479–483 (2003)
8. Gao, X.L.; Liu, J.; Zhang, L.J.; Zhang, J.X.: Effect of the overlapping factor on the microstructure and mechanical properties of pulsed Nd: YAG laser welded Ti6Al4V sheets. Mater. Charact. **93**, 136–149 (2014)
9. Anawa, E.M.; Olabi, A.G.: Optimization of tensile strength of ferritic/austenitic laser-welded components. Opt. Lasers Eng. **46**(8), 571–577 (2008)
10. Olabi, A.G.; Casalino, G.; Benyounis, K.Y.; Rotondo, A.: Minimisation of the residual stress in the heat affected zone by means of numerical methods. Mater. Des. **28**(8), 2295–2302 (2007)
11. Anawa, E.M.; Olabi, A.G.: Effects of laser welding conditions on toughness of dissimilar welded components. Appl. Mech. Mater. **5**, 375–380 (2006)
12. Anawa, E.; Olabi, A.: Developing and optimization models for multi-mechanical properties of dissimilar laser welding joints. In: Design and Computation of Modern Engineering Materials, pp. 273–285 (2014)
13. Zhang, X.; Ashida, E.; Shono, S.; Matsuda, F.: Effect of shielding conditions of local dry cavity on weld quality in underwater Nd: YAG laser welding. J. Mater. Process. Technol. **174**, 34–41 (2006)
14. Zhang, X.; Chen, W.; Ashida, E.; Matsuda, F.: Relationship between weld quality and optical emissions in underwater Nd: YAG laser welding. Opt. Lasers Eng. **41**(5), 717–730 (2004)
15. Mullick, S.; Madhukar, Y.K.; Roy, S.; Kumar, S.; Shukla, D.K.; Nath, A.K.: Development and parametric study of a water-jet assisted underwater laser cutting process. Int. J. Mach. Tools Manuf. **68**, 48–55 (2013)
16. Sun, Z.; Ion, J.C.: Laser welding of dissimilar metal combinations. J. Mater. Sci. **30**(17), 4205–4214 (1995)
17. Sun, Z.; Kuo, M.: Bridging the joint gap with wire feed laser welding. J. Mater. Process. Technol. **87**, 213–222 (1999)
18. Wang, H.M.; Chen, Y.L.; Yu, L.G.: 'In-situ' weld-alloying/laser beam welding of SiCp/6061Al MMC. Mater. Sci. Eng. A **293**, 1–6 (2000)
19. Mai, T.A.; Spowage, A.C.: Characterisation of dissimilar joints in laser welding of steel-kovar, copper-steel and copper-aluminium. Mater. Sci. Eng. A **374**, 224–233 (2004)
20. Moosavy, H.N.; Aboutalebi, M.R.; Seyedein, S.H.; Goodarzi, M.; Khodabakhshi, M.; Mapelli, C.; Barella, S.: Modern fiber laser beam welding of the newly-designed precipitation-strengthened nickel-base superalloys. Opt. Laser Technol. **57**, 12–20 (2014)
21. Cheng, P.J.; Lin, S.C.: An analytical model for the temperature field in the laser forming of sheet metal. J. Mater. Process. Technol. **101**, 260–267 (2000)
22. Serizawa, H.; Mori, D.; Shirai, Y.; Ogiwara, H.; Mori, H.: Weldability of dissimilar joint between F82H and SUS316L under fiber laser welding. Fusion Eng. Des. **88**(9), 2466–2470 (2013)
23. Çam, G.; Koçak, M.: Progress in joining of advanced materials: part 1: solid state joining, fusion joining, and joining of intermetallics. Sci. Technol. Weld. Join. **3**(3), 105–126 (1998)
24. Cam, G.; dos Santos, J.F.; Kocak, M.; Fischer, A.; Ratjen, R.: Properties of laser beam welded superalloys Inconel 625 and 718. In: European conference on laser treatment of materials, pp. 333–338 (1998)
25. Odabaşı, A.; Ünlü, N.; Göller, G.; Eruslu, M.N.: A study on laser beam welding (LBW) technique: effect of heat input on the microstructural evolution of superalloy Inconel 718. Metall. Mater. Trans. A **41**(9), 2357–2365 (2010)
26. Khan, M.M.A.; Romoli, L.; Dini, G.: Laser beam welding of dissimilar ferritic/martensitic stainless steels in a butt joint configuration. Opt. Laser Technol. **49**, 125–136 (2013)
27. Xie, M.X.; Zhang, L.J.; Zhang, G.F.; Zhang, J.X.; Bi, Z.Y.; Li, P.C.: Microstructure and mechanical properties of CP-Ti/X65 bimetallic sheets fabricated by explosive welding and hot rolling. Mater. Des. **87**, 181–197 (2015)
28. Zhang, L.J.; Zhang, G.F.; Ning, J.; Zhang, X.J.; Zhang, J.X.: Microstructure and properties of the laser butt welded 1.5-mm thick T2 copper joint achieved at high welding speed. Mater. Des. **88**, 720–736 (2015)
29. Zhang, L.J.; Zhang, G.F.; Bai, X.Y.; Ning, J.; Zhang, X.J.: Effect of the process parameters on the three-dimensional shape of molten pool during full-penetration laser welding process. Int. J. Adv. Manuf. Technol. 1–14 (2016). doi:10.1007/s00170-015-8249-x